Deep Space 1 Mission and Observation of Comet Borrellly

Meemong Lee, Richard J. Weidner
Jet Propulsion Laboratory, Pasadena, California 91109, USA
and
Laurence A. Soderblom
United States Geological Survey, Flagstaff, Arizona, 86001, USA

Introduction

The NASA's New Millennium Program (NMP) focuses on testing high-risk, advanced technologies in space with low-cost flights. The objective of the NMP technology validation missions is to enable future science missions. Thus the NMP missions themselves are technology-driven, with the principal requirements coming from the needs of the advanced technologies that form the "payload." The first NMP mission, Deep Space 1 (DS1), was launched in October, 1998. During the primary mission that ended in April, 1999, DS1 validated twelve advanced technologies [1].

After DS1 1 completed its successful primary mission in 1999, NASA sent it on a risky and ambitious extended mission to conduct comet science. In September 2001, DS1 executed a flawless encounter with comet Borrelly, yielding the best pictures and other scientific data ever collected at a comet, providing scientists with a tremendous advance in our understanding of these intriguing and important parts of the solar system.

The rich science-return was enabled by several break-through technologies including autonomous optical navigation (AutoNav), miniature integrated camera and spectrometer (MICAS), on-board data processing, model-based science observation sequence planning, and science information analysis. Digital image/signal processing was a critical element of the mission for verifying the spacecraft's orientation, tracking the encounter target, calibrating the instrument, processing the data, and analyzing the observed phenomena.

MICAS was originally equipped with four types of sensors, a CCD (charge-coupled device), an APS (active pixel sensor), a near IR (infra red) and a UV (ultra violet). Except the UV sensor that became defective during the flight calibration, MICAS was fully operational throughout the entire mission. MICAS-CCD was extensively used by AutoNav to obtain optical data to update its trajectory knowledge throughout most of the primary mission and the extended mission.

After the failure of SRU (Stellar Reference Unit) on November 11, 1999, MICAS-CCD was also used to observe the stars so that the spacecraft attitude can be controlled for communicating with the Earth and thrusting toward the comet Borrelly [2]. Employing MICAS as the only guidance for the entire extended mission was an extremely challenging task for the DS1 mission operation teams including optical navigation team, attitude control team, and science team. This paper describes a few notable challenges with respect to flight calibration, on-board data processing, and science information analysis.

MICAS calibration

MICAS is an instrument system that integrates four types of sensors (CCD, APS, IR, UV), via a shared optical structure and a common electronics interface. Several flight calibration scenarios were designed and performed utilizing various natural targets available on the way to the encounter targets. MICAS structure provided a few special features to assist flight calibration process as well as to enhance science return.

The IR and UV detectors were divided into two areas, a key-hole and a slit. The key-hole was for observing a point source while the slit was for observing an extended target while the spacecraft slews around the target (i.e., pushbroom operation). The size of the key-hole area was determined to be 0.1 deg to compensate for the estimated pointing error (0.03 deg) while observing a point source.

A separate optical port was created with a diffusor so that the Sun can be utilized as a natural flat field for the sensitivity calibration. Unfortunately, during the mission operation, it was discovered that the desired orientation for pointing the diffusor at the Sun endangered the star tracking ability. The Jupiter was used as an alternative target and the spatial variation was analyzed by orienting the spacecraft system so that the apparent location of the Jupiter forms a two dimensional grid on the detector frame. A bright star and a patch of dark sky were used for defocusing and dark current property modeling.

MICAS was body-mounted on the DS1, requiring spacecraft's attitude change for each target viewing. Thus, the geometric alignment of MICAS with respect to the spacecraft and the performance properties (e.g., turn and slew) of the attitude control subsystem (ACS) had to be accurately modeled. Figure 1 illustrates two APS observations where the spacecraft was

commanded to point at the planet Mars and slowly slew around it horizontally and vertically. The apparent orientation of the intensity profile was used to model the geometric alignment and the center location and trailing intensity profile were the pointing used to model the performance of the attitude control subsystem.

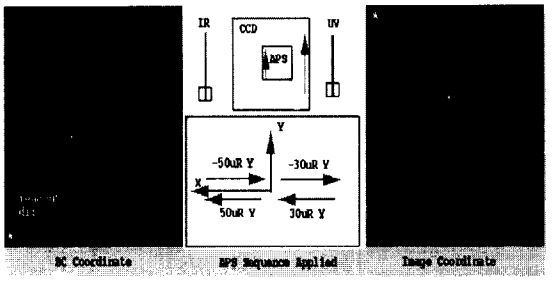

Figure 1 Geometric alignment verification

During the flight calibration process, it was discovered that MICAS suffers from both internal and external background noise and a significant effort was made to characterize them. The background noise was from the sun light bounced off of the solar panel and penetrated through the solar port. The stray light casted two distinctive noise patterns depending on the relative sun light direction. The background noise became a significant challenge for the optical navigation team who needed to observe faint star with long exposure durations [2].

The two types of stray light patterns mentioned above can be seen in Figure 1 (blow torch like shape) and Figure 2 (diffused solar panel shape). The blow-torch-noise couldn't be coped with a data processing method due to the signal loss from the intensity saturation. An extensive calibration process was designed and performed to determine the safe solar cone angle range for MICAS observation. The diffused solar-panel-shape noise was observed when the solar cone angle was high. In order to remove the background noise, image differencing between two images with a slightly different pointing, was applied (see Figure 2).

On-board Data Processing

In order to maximize the science return, the operation planning started at the design phase of the mission. The operation plan was virtually executed based on the subsystem property models. Figure 3 illustrates an example of virtual encounter scenario exercise. Several subsystem design changes were made based on the virtual execution results.

The design change included extended target tracking by AutoNav, adding 32 MB internal buffer to MICAS, providing on-board data processing capabilities including data compression sub-area extraction, and automated target area extraction. The internal buffer enabled pushbroom observation (successive multiple exposure) and near encounter observations. The on-board data processing capabilities more than tripled the amount of science data products received.

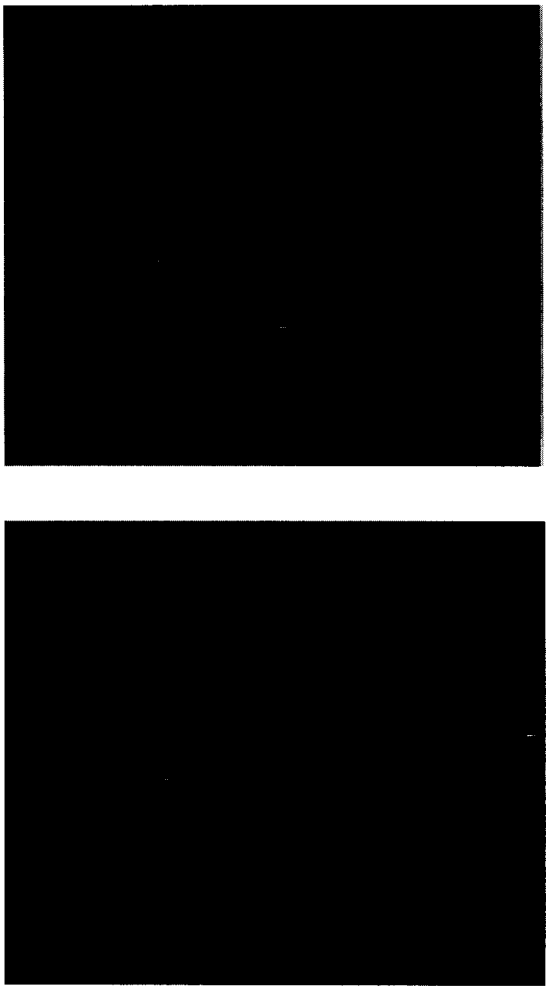

Figure 2 Stray light example before and after background noise removal process

The MICAS data compression implementation was based on a reversible integer wavelet transform filter developed at JPL [3]. Three types of compression options were provided: lossless option for data reduction without losing the quality, lossy option for precise data volume control by specifying the desired compression rate, progressive option for selective transmission after browsing the low resolution image. The lossless option was employed for most of the CCD image frames and IR slit images averaging 3:1 compression rate. The lossy and progressive options

were applied to only non-scientific observation image frames.

The sub-area extraction was applied to all of the IR-keyhole images, extracting the first 50 lines from the 264 lines of IR detector frame. This capability significantly contributed acquiring IR observations enabling a super-resolution material identification of Mars atmospheric layer, asteroid Braille, and comet Borrelly. The automated target area extraction, which requires a well defined size and brightness threshold, couldn't be applied due to the unexpected background noise discussed above.

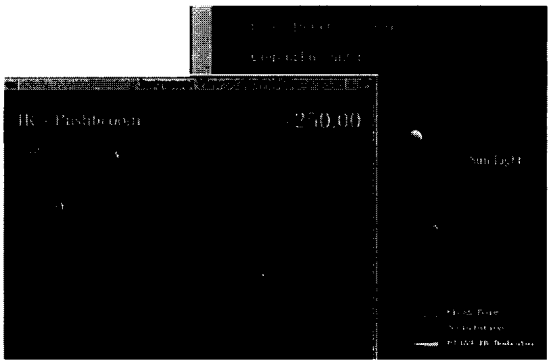

Figure 3 Virtual Execution of Asteroid Encounter

Science Analysis [5]

During the comet Borrelly encounter, 24 IR keyhole images and 6 CCD images (5 from the medium range encounter and 1 from the near encounter) were successfully acquired. In the CCD images, two types of blurring were present, optical blurring and motion blurring. In order to restore the blurred image, A deblurring process developed at JPL based on the maximum likely hood algorithm was employed with a blurring kernel constructed for each image. The blurring kernel was created by constructing a two dimensional motion template and convolving it with the point spread function of MICAS.

Figures 4 and 5 show before and after debluring process applied to the two highest resolution images. When the motion is slight (Figure 4) the restoration could be achieved within 20 iterations. When the motion is significant (Figure 5) the restoration required more than 40 iterations. In order to cope with the variable speed in the motion as shown in Figure 5, it was necessary to modify the motion template with the estimated speed profile.

The comet Borrelly was at 1.36 AU from the Sun, about 10 days after the comet's perihelion. The baseline plan was for the spacecraft to pass at 17 km/s about 2000 km from the nucleus on the Sun-nucleus line. With a period of 6.9 years, this Jupiter-family comet has been extensively studied by many investigators; it is moderately active with a well-defined coma and tails. The morphological surface features of the nucleus of Borrelly was defined from the two highest resolution (47-to-58 m/pixel) images discussed above.

A three-dimensional model of Borrelly's nucleus was constructed by applying a stereogrammetric analysis on the two highest-resolution stereo pair (shown above). Although the convergence angle between the two is only 4.4°, this pair best shows the smallest detail visible on the nucleus (ranges 3960 and 3560 km with resolutions of 52 and 47 m/pixel and phase angles of 56.0° and 51.6°). The three-dimensional model is shown in Figure 6. Left is a map of range from the spacecraft to the surface for the highest resolution image (left image in fig. 3). Right side is a perspective view in the direction shown elevated 45° out-of-plane. Colors: 200-m range contours.

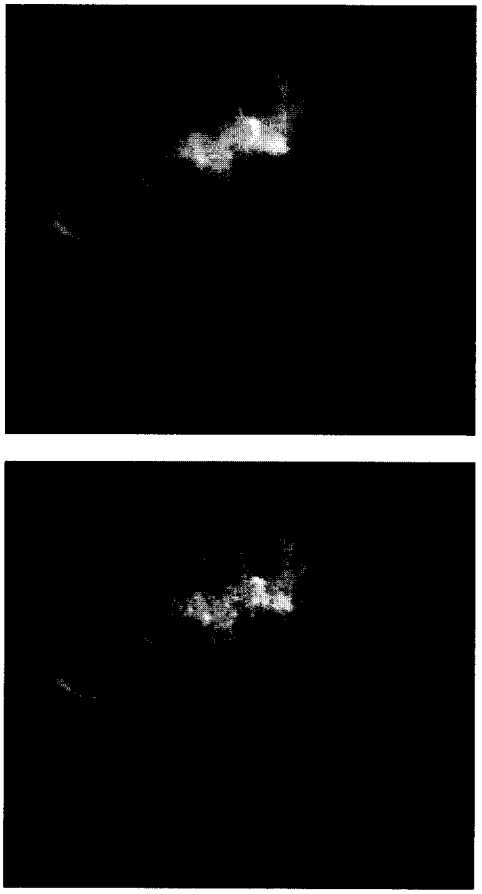

Figure 4 Highest resolution comet image (above: raw, below: restored)

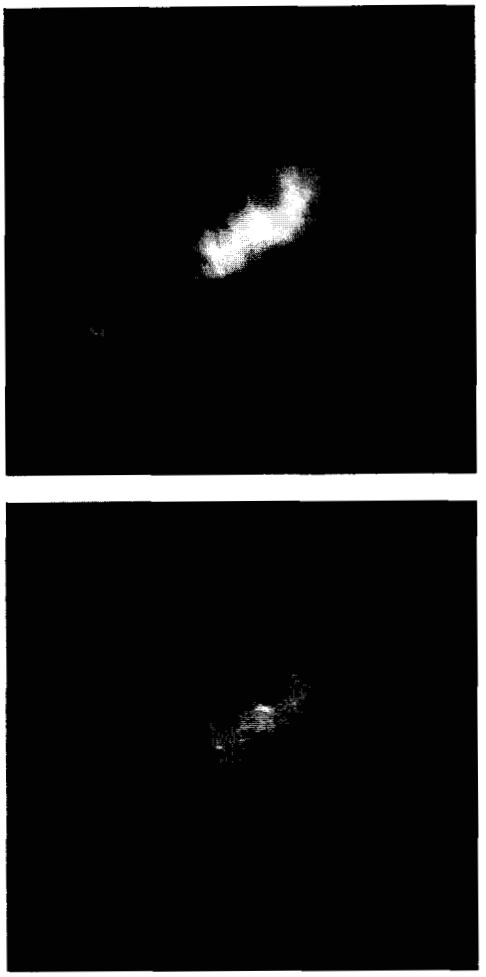

Figure 5 Motion blurred image before and after restoration

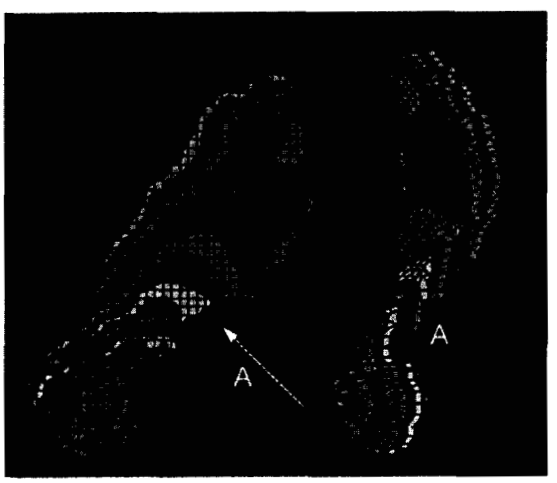

Figure 6 Three Dimensional Model of the Nucleus

As shown in Figure 7, short-wavelength infrared spectra of the nucleus have a 2.39-μm absorption feature. Spectra are normalized at 2.359 μm and incrementally offset from one another by 0.02. The empty space in the central part of the plot indicates the lack of data due to the instrument saturation. Two smooth curves at the top and bottom indicate the model temperature profile and the SWIR data appear to fit within the expected range.

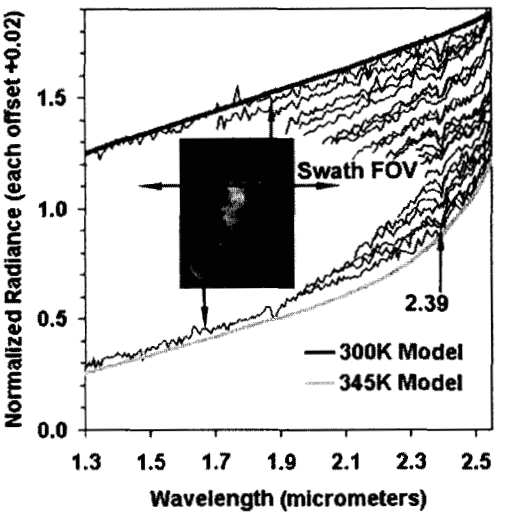

Figure 7 Short-waevlength Infrared Spectra of the Nucleus

References

.[1] Rayman, M., "The Deep Space 1 Extended Mission", Acta Astronautica Vol. 48 No 5-12, pp 693-705

[2] Deep Space Technology Validation Report, JPL Pulibcation 00-10 (Jet Propulsion Laboratory, Pasadena, CA)

[3] Lee, M. et al, "Mission Lifecycle Modeling and Simulation", IEEE Aeroconference, Big Sky, Montana, 2000

[4] Majani, E, "A Reversible Integer Wavelet Transform and Progressive Data Compression", IEEE Data Compression Conference, Snowbird, Utah, 1996

[5] Soderblom, L. et al, "Observations of Comet 19P/Borrelly by the Miniature Integrated Camera and Spectroneter aboard Deep Space 1", Science, Vol. 296, p1087-1090